

# Supplemental Material to "An individual Cr atom in a semiconductor quantum dot: optical addressability and spin-strain coupling"

A. Lafuente-Sampietro,<sup>1, 2, 3</sup> H. Utsumi,<sup>3</sup> H. Boukari,<sup>1, 2</sup> S. Kuroda,<sup>3</sup> and L. Besombes<sup>1, 2</sup>

<sup>1</sup>Université Grenoble Alpes, Institut Néel, F-38000 Grenoble, France

<sup>2</sup>CNRS, Institut Néel, F-38000 Grenoble, France

<sup>3</sup>Institute of Material Science, University of Tsukuba, Japan

In this supplemental material, we first describe the influence of strain on the fine structure of a Cr atom embedded in a II-VI zinc-blende semiconductor. We then present the complete electron-hole-Cr spin effective Hamiltonian used to model a low symmetry singly Cr-doped II-VI quantum dot. We finally present additional data on Cr-doped quantum dots: the temperature dependence of the PL of X-Cr and some statistics on the energy splitting of X-Cr and X<sup>2</sup>-Cr.

## CR ENERGY LEVELS IN A II-VI SEMICONDUCTOR

Cr atoms are incorporated into II-VI semiconductors as Cr<sup>2+</sup> ions on cation sites forming a deep impurity level. The ground state of a free Cr<sup>2+</sup> is <sup>5</sup>D with the orbital quantum number L=2 and a spin S=2 yielding a 25-fold degeneracy. In the crystal field of T<sub>d</sub> symmetry of the tetrahedral cation site in zinc-blende crystal, the degeneracy is partially lifted (see Fig. 1): the <sup>5</sup>D term splits into 15-fold degenerate orbital triplet <sup>5</sup>T<sub>2</sub> and 10-fold degenerate orbital doublet <sup>5</sup>E. The Jahn-Teller distortion reduces the symmetry to D<sub>2d</sub> and leads to a splitting of the <sup>5</sup>T<sub>2</sub> ground state into a 5-fold degenerate <sup>5</sup>B<sub>2</sub> orbital singlet and a <sup>5</sup>E orbital doublet.

The ground state orbital singlet <sup>5</sup>B<sub>2</sub> is further split by the spin-orbit interaction. In a strain free crystal, it was found that the ground state splitting can be described by the spin effective Hamiltonian [1]:

$$\mathcal{H}_{Cr,CF} = D_0 S_z^2 + \frac{1}{180} F [35S_z^2 - 30S(S+1)S_z^2 + 25S_z^2] + \frac{1}{6} a [S_1^4 + S_2^4 + S_3^4] \quad (1)$$

with the Cr spin S=2 and |D<sub>0</sub>| ≈ |a|, |F|. In the model presented here, we use a = 0 and F = 0. The x, y, z principal axes were found to coincide with the cubic axes (1,2,3) giving rise to three identical sites, each given by (1) but with the z axis of each along a different cubic axis (1,2,3). A value of D<sub>0</sub> ≈ +30μeV was estimated from Electron Paramagnetic Resonance (EPR) measurements in highly diluted bulk (Cd,Cr)Te [1].

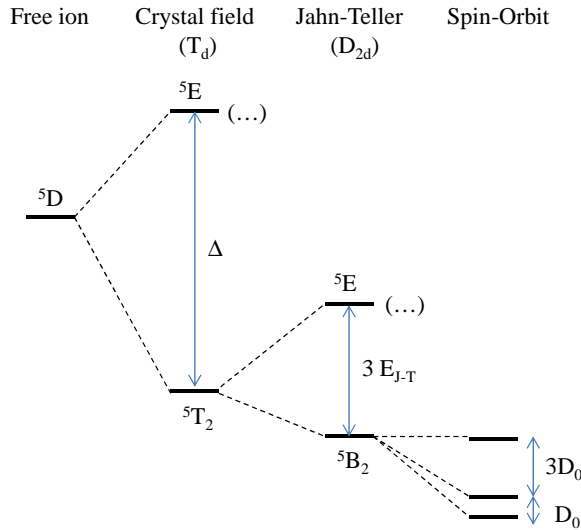


FIG. 1: Scheme of the energy level splitting of Cr<sup>2+</sup> at a cation site in II-VI compounds having zinc blende structure (T<sub>d</sub>) with a crystal field parameter  $\Delta$ , a Jahn-Teller energy  $E_{J-T}$  and a spin-orbit level spacing  $D_0$ .

Static biaxial compressive strain in the (001) plane, as observed in self-assembled quantum dots, reduces the symmetry to D<sub>2d</sub> and destabilize the Cr 3d orbitals  $d_{xz}$  and  $d_{yz}$  having an electron density pointing along the [001]

axis ( $z$  axis). The Cr ground state is then a 5-fold degenerated orbital singlet formed from the  $d_{xy}$  orbital. It corresponds to the Jahn-Teller ground state with a tetragonal distortion along the [001] axis [2].

An applied stress will also influence the Cr spin fine structure splitting through the modification of the crystal field and the spin-orbit interaction [1]. For an arbitrary strain tensor, the general form of the Cr ground state spin effective Hamiltonian is

$$\mathcal{H}_{Cr,\varepsilon} = c_1 e_A S_\theta + c_2 e_\theta S_\theta + c_3 e_\epsilon S_\epsilon + c_4 e_\zeta S_\zeta + c_5 (e_\xi S_\xi + e_\eta S_\eta) \quad (2)$$

with  $S_i$  defined as:

$$\begin{aligned} S_\theta &= S_z^2 - \frac{1}{2}[S_x^2 + S_y^2] \\ S_\epsilon &= \frac{1}{2}\sqrt{3}[S_x^2 - S_y^2] \\ S_\xi &= S_y S_z + S_z S_y \\ S_\eta &= S_x S_z + S_z S_x \\ S_\zeta &= S_x S_y + S_y S_x \end{aligned} \quad (3)$$

and  $e_i$  defined similarly as:

$$\begin{aligned} e_\theta &= \varepsilon_{zz} - \frac{1}{2}[\varepsilon_{xx} + \varepsilon_{yy}] \\ e_\epsilon &= \frac{1}{2}\sqrt{3}[\varepsilon_{xx} - \varepsilon_{yy}] \\ e_\xi &= \varepsilon_{yz} + \varepsilon_{zy} \\ e_\eta &= \varepsilon_{xz} + \varepsilon_{zx} \\ e_\zeta &= \varepsilon_{xy} + \varepsilon_{yx} \\ e_A &= \varepsilon_{xx} + \varepsilon_{yy} + \varepsilon_{zz} \end{aligned} \quad (4)$$

For flat self-assembled quantum dots with dominant large biaxial strain we have a strain tensor:

$$\varepsilon_{ij} = \begin{pmatrix} \varepsilon_{\parallel} & 0 & 0 \\ 0 & \varepsilon_{\parallel} & 0 \\ 0 & 0 & \varepsilon_{zz} \end{pmatrix} \quad (5)$$

with

$$\varepsilon_{zz} = -2 \frac{C_{11}}{C_{12}} \varepsilon_{\parallel} \quad (6)$$

where  $C_{11} \approx 5.4 \cdot 10^{10} Pa$  and  $C_{12} \approx 3.7 \cdot 10^{10} Pa$  are the elastic constants of CdTe [3]. For this strain configuration, the Cr fine structure is controlled by the spin-lattice coupling coefficients  $c_1$  (symmetric coefficient) and  $c_2$  (tetragonal coefficients). Strain-coupling coefficients estimated from EPR measurements in bulk Cr doped CdTe are listed in table I.

TABLE I: Values for spin to strain coupling coefficients of Cr in bulk CdTe (in meV) extracted from ref.[1].

$c_1$	$c_2$	$c_3$	$c_4$	$c_5$
$-0.25 \pm 2$	$+4.9 \pm 2$	$-1.25 \pm 0.5$	$+4.9 \pm 2$	$+3.7 \pm 1.25$

For a pure CdTe layer lattice matched on ZnTe, we have  $\varepsilon_{\parallel} = (a_{ZnTe} - a_{CdTe})/a_{CdTe} \approx -5.8\%$  with  $a_{CdTe} = 6.48 \text{\AA}$  and  $a_{ZnTe} = 6.10 \text{\AA}$ . The strain controlled part of the spin Hamiltonian  $\mathcal{H}_{Cr,\varepsilon}$  becomes:

$$\mathcal{H}_{Cr,\varepsilon_{||}} = \frac{3}{2}\varepsilon_{||}[2c_1(1 - \frac{C_{12}}{C_{11}}) - c_2(1 + 2\frac{C_{12}}{C_{11}})]S_z^2 = D_0 S_z^2 \quad (7)$$

where we can estimate  $D_0 \approx 1 \pm 0.6$  meV from the values of the spin-strain coupling coefficients in CdTe (table I). However one should note the quantum dots could be partially relaxed and may contain a significant amount of Zn. We were not able to find spin to strain coupling coefficients for Cr in ZnTe and (Cd,Zn)Te alloy in literature. A value of  $D_0 \approx +280\mu\text{eV}$ , much larger than for CdTe, was however estimated in strain-free Cr-doped bulk ZnTe [1]. Larger spin-strain coupling coefficients could then be expected for Cr in ZnTe and (Cd,Zn)Te alloys.

Finally, an anisotropy of the strain in the quantum dot plane (001) with principal axis along [010] or [100] axes ( $\varepsilon_{xx} \neq \varepsilon_{yy}$  and  $\varepsilon_{xy}=\varepsilon_{yx}=0$ ) would affect the Cr fine structure through the tetragonal coefficient  $c_3$ . This coupling can be described by an additional term in the spin-strain Hamiltonian

$$\mathcal{H}_{Cr,\varepsilon_{\perp}} = \frac{3}{4}c_3(\varepsilon_{xx} - \varepsilon_{yy})(S_x^2 - S_y^2) = E(S_x^2 - S_y^2) \quad (8)$$

This anisotropy term  $E$  couples Cr spin states separated by two units and in particular  $S_z=+1$  to  $S_z=-1$  which are initially degenerated. It could be exploited to induce a large strain mediated coherent coupling between a mechanical oscillator and the Cr spin [4].

## OPTICAL TRANSITIONS IN A CR-DOPED QUANTUM DOT

The complete electron-hole-Cr Hamiltonian in self-assembled quantum dot ( $\mathcal{H}_{X-Cr}$ ) can be separated into six parts:

$$\mathcal{H}_{X-Cr} = \mathcal{H}_{Cr,\varepsilon} + \mathcal{H}_{c-Cr} + \mathcal{H}_{mag} + \mathcal{H}_{e-h} + \mathcal{H}_{band} + \mathcal{H}_{scat} \quad (9)$$

$\mathcal{H}_{Cr,\varepsilon}$  describes the fine structure of the Cr atom and its dependence on local strain as presented in the previous section.

$\mathcal{H}_{c-Cr}$  describes the coupling of the electron and hole with the Cr spin. It reads

$$\mathcal{H}_{c-Cr} = I_{eCr} \vec{S} \cdot \vec{\sigma} + I_{hCr} \vec{S} \cdot \vec{J} \quad (10)$$

with  $I_{eCr}$  and  $I_{hCr}$  the exchange integrals of the electron ( $\vec{\sigma}$ ) and hole ( $\vec{J}$ ) spins with the Cr spin ( $\vec{S}$ ).

An external magnetic field couples via the standard Zeeman terms to both the Cr spin and carriers spins and a diamagnetic shift of the electron-hole pair can also be included resulting in

$$\mathcal{H}_{mag} = g_{Cr}\mu_B \vec{B} \cdot \vec{S} + g_e\mu_B \vec{B} \cdot \vec{\sigma} + g_h\mu_B \vec{B} \cdot \vec{J} + \gamma B^2 \quad (11)$$

The electron-hole exchange interaction,  $\mathcal{H}_{e-h}$ , contains the short range and the long range parts. The short range contribution is a contact interaction which induces a splitting  $\delta_0^{sr}$  of the bright and dark excitons and, in the reduced symmetry of a zinc-blend crystal ( $T_d$ ), a coupling  $\delta_2^{sr}$  of the two dark excitons. The long range part also contributes to the bright-dark splitting by an energy  $\delta_0^{lr}$ . In quantum dots with  $C_{2v}$  symmetry (ellipsoidal flat lenses for instance [5]) the long range part also induces a coupling  $\delta_1$  between the bright excitons. Realistic self-assembled quantum dots have symmetries which can deviate quite substantially from the idealized shapes of circular or ellipsoidal lenses. For a  $C_s$  symmetry (truncated ellipsoidal lens), additional terms coupling the dark and the bright excitons have to be included in the electron-hole exchange Hamiltonian. Following Ref. [5], the general form of the electron-hole exchange Hamiltonian in the heavy-hole exciton basis  $|+1\rangle, |-1\rangle, |+2\rangle, |-2\rangle$  for a low symmetry quantum dot ( $C_s$ ) is

$$\mathcal{H}_{e-h} = \frac{1}{2} \begin{pmatrix} -\delta_0 & e^{i\pi/2}\delta_1 & e^{i\pi/4}\delta_{11} & -e^{i\pi/4}\delta_{12} \\ e^{i\pi/2}\delta_1 & -\delta_0 & e^{-i\pi/4}\delta_{12} & -e^{-i\pi/4}\delta_{11} \\ e^{-i\pi/4}\delta_{11} & e^{i\pi/4}\delta_{12} & \delta_0 & \delta_2 \\ -e^{-i\pi/4}\delta_{12} & -e^{i\pi/4}\delta_{11} & \delta_2 & \delta_0 \end{pmatrix} \quad (12)$$

TABLE II: Values of the parameters used in the model of Cr-doped CdTe/ZnTe quantum dot presented in figure 3 of the main text. The value of the parameters not listed in the table is 0. The chosen values are typical for CdTe/ZnTe quantum dots and can be compared with parameters extracted from Mn-doped quantum dots [7, 8].

$I_{eCr}$	$I_{hCr}$	$\delta_0$	$\delta_1$	$\delta_{12}$	$\delta_{11}$	$\frac{\delta_{xz}}{\Delta_{lh}}$	$\frac{\delta_{xx,yy}}{\Delta_{lh}}$	$D_0$	$g_{Cr}$	$g_e$	$g_h$	$\gamma$	$\eta$	$T_{eff}$
$\mu eV$	$\mu eV$	$meV$	$\mu eV$	$\mu eV$	$\mu eV$			$meV$				$\mu eV/T^2$	$\mu eV$	K
-70	-280	-1	250	150	50	0.05	0.05	2.5	2	-0.7	0.4	1.5	25	25

The terms  $\delta_{11}$  and  $\delta_{12}$ , not present in symmetry  $C_{2v}$ , give an in-plane dipole moment to the dark excitons [6]. The term  $\delta_{12}$  which couples  $|\pm 1\rangle$  and  $|\mp 2\rangle$  excitons respectively is responsible for the dark-bright anti-crossing observed on the low energy side of the emission of Cr-doped quantum dots.

The band Hamiltonian,  $\mathcal{H}_{band} = E_g + \mathcal{H}_{vbm}$ , stands for the energy of the electrons (i.e. the band gap energy  $E_g$ ), and the heavy-holes (hh) and light-holes (lh) energies ( $\mathcal{H}_{vbm}$ ) [7, 8]. To describe the influence of a reduced symmetry of the quantum dot on the valence band, we considered here the four lowest energy hole states  $|J, J_z\rangle$  with angular momentum  $J = 3/2$ . A general form of Hamiltonian describing the influence of shape or strain anisotropy on the valence band structure can be written in the basis  $(|\frac{3}{2}, +\frac{3}{2}\rangle, |\frac{3}{2}, +\frac{1}{2}\rangle, |\frac{3}{2}, -\frac{1}{2}\rangle, |\frac{3}{2}, -\frac{3}{2}\rangle)$  as:

$$\mathcal{H}_{vbm} = \begin{pmatrix} 0 & -Q & R & 0 \\ -Q^* & \Delta_{lh} & 0 & R \\ R^* & 0 & \Delta_{lh} & Q \\ 0 & R^* & Q^* & 0 \end{pmatrix} \quad (13)$$

with

$$Q = \delta_{xz} - i\delta_{yz}; R = \delta_{xx,yy} - i\delta_{xy} \quad (14)$$

Here, R describes the heavy-hole / light-hole mixing induced by an anisotropy in the quantum dot plane  $xy$  and Q takes into account an asymmetry in the plane containing the quantum dot growth axis  $z$ . The reduction of symmetry can come from the shape of the quantum dot (Luttinger Hamiltonian) or the strain distribution (Bir and Pikus Hamiltonian).  $\Delta_{lh}$  is the splitting between lh and hh which is controlled in quantum dots both by the in-plane biaxial strain and the confinement.

Considering only an in-plane anisotropy (Q=0), it follows from (13) that the valence band mixing couples the heavy-holes  $J_z = \pm 3/2$  and the light-holes  $J_z = \mp 1/2$  respectively. For such mixing, the isotropic part of the short range exchange interaction, which can be written in the form  $2/3\delta_0^{sr}(\vec{\sigma} \cdot \vec{J})$ , couples the two bright excitons. This mixing is also responsible for a weak  $z$ -polarized dipole matrix element of the dark excitons coming from the light-hole part of the hole wave function.

A deformation in a vertical plane (Q term) couples the heavy-holes  $J_z = \pm 3/2$  and the light-holes  $J_z = \pm 1/2$  respectively. In this case, the short range electron-hole exchange interaction couples  $|+1\rangle$  and  $|+2\rangle$  exciton on one side and  $| -1\rangle$  and  $| -2\rangle$  exciton on the other side.

For a general description and as it was observed in Mn-doped quantum dots [8–10], we can also take into account the perturbation of the wave function of the exciton in the initial state of the optical transition by the hole-Cr exchange interaction. This perturbation depends on the value of the exchange energy between the Cr spin  $S_z$  and the hole spin  $J_z$  and can be represented, using second order perturbation theory, by an effective spin Hamiltonian [8–10]

$$\mathcal{H}_{scat} = -\eta S_z^2 \quad (15)$$

with  $\eta > 0$ .

Using the Hamiltonian of the excited state  $\mathcal{H}_{X-Cr}$  and the Hamiltonian of the ground state

$$\mathcal{H}_{Cr} = \mathcal{H}_{Cr,\epsilon} + g_{Cr}\mu_B \vec{B} \cdot \vec{S} \quad (16)$$

we can compute the spectrum of a quantum dot containing a Cr atom. The occupation of the X-Cr levels is described by an effective spin temperature  $T_{eff}$  and the optical transitions probabilities are obtained calculating the matrix

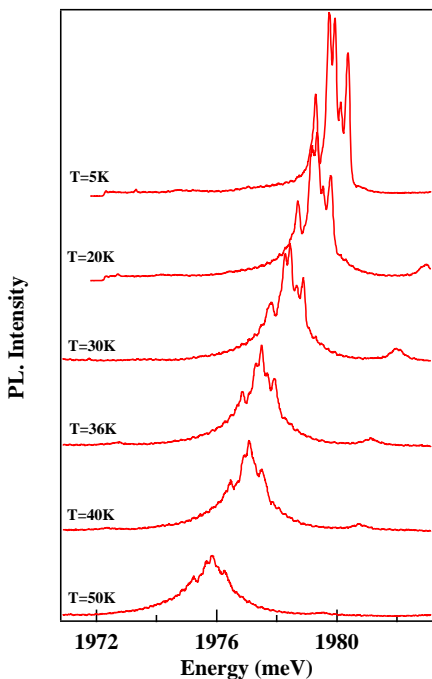


FIG. 2: Temperature dependence of the photoluminescence of X-Cr in a Cr-doped QD (QD4 in the main text).

elements  $|\langle S_z | X, S_z \rangle|^2$  where  $X$  and  $S_z$  stands for the 8 possible exciton states and the Cr spin respectively. The resulting photoluminescence spectra calculated with the parameters listed in table II are presented in figure 3 of the main text.

#### COMPLEMENTARY DATA ON PHOTOLUMINESCENCE OF CR-DOPED QUANTUM DOTS

The temperature dependence of the X-Cr emission in QD4 at zero magnetic field is presented in figure 2. With the increase of the temperature, we observe a significant line broadening induced by the interaction with acoustic phonons. In the investigated temperature range where we still obtain a significant PL intensity and resolved PL lines (below  $T=50\text{K}$ ), no contribution of the  $S_z=\pm 2$  Cr spins states are observed in the emission of the exciton.

Figure 3 presents some statistics on the values of the overall energy splitting of X-Cr ( $\Delta X$ ) and  $\text{X}^2\text{-Cr}$  ( $\Delta X^2$ ) obtain on 12 Cr-doped quantum dots. For most of the investigated dots,  $\Delta X$  remains below 1 meV and  $\Delta X^2$  is also smaller than  $\Delta X$  suggesting an interaction between the Cr spin and the biexciton.

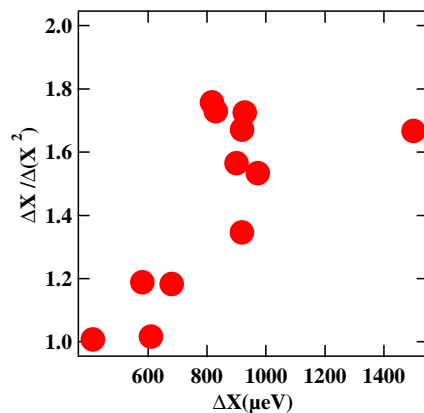


FIG. 3: Ratio of the overall splitting (i.e energy difference between the two extreme bright exciton lines) of  $\text{X}^2\text{-Cr}$  and X-Cr as a function of the splitting of X-Cr for 12 different Cr-doped QDs.

- 
- [1] J.T. Vallin and G.D. Watkins, Phys. Rev. B **9**, 2051 (1974).
  - [2] M. Brousseau, Les defauts ponctuels dans les semiconducteurs, Les Editions de Physiques (1988).
  - [3] R.D. Greenough, S.B. Palmer, J. Phys. D **6**, 586 (1973).
  - [4] P. Ovartchaiyapong, K. W. Lee, B. A. Myers, A. C. Bleszynski Jayich, Nature Communication **5**, 4429 (2014).
  - [5] M. Zielinski, Y. Don and D. Gershoni, Phys. Rev. B **91**, 085403 (2015).
  - [6] M. Bayer, G. Ortner, O. Stern, A. Kuther, A.A. Gorbunov, A. Forchel, P. Hawrylak, S. Fafard, K. Hinzer, T.L. Reinecke, S.N. Walck, J.P. Reithmaier, F. Klopf, F. Schafer, Phys. Rev. B **65**, 195315 (2002).
  - [7] Y. Leger, L. Besombes, L. Maingault, H. Mariette, Phys. Rev. B **76**, 045331 (2007).
  - [8] B. Varghese, H. Boukari, L. Besombes, Phys. Rev. B **90**, 115307 (2014).
  - [9] L. Besombes, Y. Leger, L. Maingault, D. Ferrand, H. Mariette, J. Cibert, Phys. Rev. B **71**, 161307(R) (2005).
  - [10] A. H. Trojnar, M. Korkusinski, U. C. Mendes, M. Goryca, M. Koperski, T. Smolenski, P. Kossacki, P. Wojnar, P. Hawrylak, Phys. Rev. B **87**, 205311 (2013).